The Effect of Pre-Main Sequence Stars on Star Cluster Dynamics

Robert Wiersma [1], Alison Sills [2] and Simon Portegies Zwart [3]

ABSTRACT

We investigate the effects of the addition of pre-main sequence evolution to star cluster simulations. We allowed stars to follow pre-main sequence tracks that begin at the deuterium burning birthline and end at the zero age main sequence. We compared our simulations to ones in which the stars began their lives at the zero age main sequence, and also investigated the effects of particular choices for initial binary orbital parameters. We find that the inclusion of the pre-main sequence phase results in a slightly higher core concentration, lower binary fraction, and fewer hard binary systems. In general, the global properties of star clusters remain almost unchanged, but the properties of the binary star population in the cluster can be dramatically modified by the correct treatment of the pre-main sequence stage.

Subject headings: stars: evolution — stars: pre–main-sequence — open clusters and associations: general — galaxies: star clusters

1. Introduction

Over the past two decades, dynamical simulations of star clusters have become much more realistic. This realism takes the form of an increasingly complex treatment of individual stars in the cluster. For years, dynamical models only considered stars as single equal-mass points. The introduction of a mass function into dynamical models quickly necessitated some treatment of stellar evolution. High mass stars have much shorter lifetimes than low mass stars, mass loss from high mass stars can remove a significant fraction of the mass from the

[1]Department of Physics and Astronomy, McMaster University, Hamilton, Ontario, Canada, L8S 4M1; current address: Leiden Observatory, P.P. Box 9513, 2300 RA Leiden, Netherlands; wiersma@strw.leidenuniv.nl

[2]Department of Physics and Astronomy, McMaster University, Hamilton, Ontario, Canada, L8S 4M1; asills@mcmaster.ca

[3]Astronomical Institute "Anton Pannekoek" and Section Computational Science, University of Amsterdam, Kruislaan 403, 1098 SJ Amsterdam, Netherlands; spz@science.uva.nl

cluster, and very high mass stars can completely dominate the dynamical evolution of the cores of clusters (Elson, Hut, & Inagaki 1987; Hut et al. 2003; Portegies Zwart et al. 2004). Binary stars also have a substantial impact on the cluster dynamics, by acting as energy sinks or sources. It has been known for a long time that a single massive binary can dominate the evolution of star clusters (Aarseth 1971). A hard binary system can produce cluster energy through an encounter with another system that leaves the binary system with a tighter orbit. Encounters between soft binary systems and other objects can release the binary's binding energy to cool the cluster, whereas interactions with hard binaries effectively heat the cluster. Dynamically produced binaries were recognized as a key population for halting core collapse (Elson, Hut, & Inagaki 1987). Open clusters also have primordial binaries (Mathieu & Latham 1986; Kouwenhoven et al. 2005, e.g.), and those binary systems can affect the cluster evolution from its birth.

Stellar dynamicists realized that the point mass approximation for stars was neglecting a number of dynamically significant processes in clusters. Allowing stars to have radii that change as they evolve was an important next addition to stellar dynamics simulations (Portegies Zwart et al. 2001; Hurley et al. 2001; de la Fuente Marcos & de la Fuente Marcos 2002). Finite stellar radii are most important for two aspects of these simulations. First, binary stars can undergo mass transfer as one member of the system fills its Roche lobe, either through evolution of the star or dynamical modification of the orbital parameters of the system. Changing binary systems will change how the binaries affect the evolution of the cluster. In the extreme case, the two components of the binary system can merge. Secondly, stars with finite radii can collide with other stars, either through direct hyperbolic collisions (in dense clusters) or in highly eccentric binary systems created after close encounters. One of the earliest papers to show the dynamical importance of binary-single encounters was written 30 years ago (Hills 1975). Stellar collisions can produce blue stragglers (Sills et al. 1997) and other non-standard stellar populations (Portegies Zwart et al. 1999). These populations can in turn modify the dynamical evolution of the cluster.

Young, open clusters are of particular interest when simulating star clusters. Because they tend to have a relatively small number of stars, open clusters provide observations that do not require prohibitive computational expense to reproduce. They also are well studied and the evolution of their stellar populations (population I) are well determined. Some open clusters are young enough to have pre-main sequence stars that are observable; indeed numerous authors have reported pre-main sequence stars in the Pleiades for instance (Garcia Lopez, Rebolo, & Martin 1994; Stauffer et al. 2003). For dynamicists, open clusters showcase a variety of phenomenon that play an important role in the evolution of the cluster. The environment that typifies the core of such a cluster is dense enough to provide for a rather high (and well known) binary fraction, and collisions, mergers, and other encounters

are expected. All of these factors make open clusters an excellent place to start when integrating stellar evolution with dynamics.

A number of authors have endeavored to push the limits of realism in dynamical simulations. Hurley et al. (2001) start their simulations with 10000 - 15000 stars distributed via Plummer and King models with varying fractions of binaries. They assign masses to these using stars using Kroupa, Gilmore, & Tout (1991); Kroupa, Tout, & Gilmore (1993) initial mass functions, and evolve them from the zero age main sequence using recipes detailed in Hurley, Pols, & Tout (2000). Their model includes the effects of the galactic tidal field. Because their study focused on blue stragglers, they included collisions and mergers as well as close encounters. Portegies Zwart et al. (2001) (hereafter PZ01) start with 3072 stars all distributed using a King model, and using a Scalo (1986) mass function. Their treatment of binary and stellar evolution is somewhat different from Hurley et al. (2001), and will be discussed in more detail in later sections of this paper.

All previous work assumed that all stars began their lives on the zero age main sequence. However, low mass stars make up the bulk of stars in a cluster for any reasonable initial mass function. Low mass stars also have a pre-main sequence lifetime that is a substantial fraction of the cluster lifetime, significantly influencing a cluster population. These young stars have radii which can be up to 10 times larger than their main sequence radii. Therefore, some binaries could have undergone an episode of mass transfer that was hitherto not taken into account. Also, larger stars are more likely to have experienced a collision; those collision products will have been missed in previous simulations. Including pre-main sequence evolution is regarded as a potentially important step in increasing the realism of stellar dynamics simulations (Sills et al. 2003).

In this paper, we explore the effect of including the pre-main sequence phase of stellar evolution in a stellar dynamics calculation. We look at the differences between simulations with and without the pre-main sequence in terms of global cluster properties (density profile, dissociation time, etc.) and in terms of the observable effect on the colour-magnitude diagram of the cluster. We look at the change in number and nature of unusual stellar populations and of the evolved stellar populations. In section 2, we outline the dynamical method used and how we incorporated pre-main sequence evolution. In section 3 we present our results, and discuss their implication in section 4.

2. Method

For all our simulations, we use the STARLAB software environment, featuring the `kira` integrator (McMillan 1996; Portegies Zwart et al. 2001) and `SeBa` stellar and binary evolution package (Portegies Zwart & Verbunt 1996; Portegies Zwart & Yungelson 1998). The simulations were run using the GRAPE-6 hardware (Makino et al. 2003).

2.1. Initial Conditions

In the interests of simulating observable results, we choose parameters corresponding to population I, young clusters. These clusters typically have approximately 1000 stars, and are no older than a few billion years.

We ran three sets of three simulations with different realizations of the input parameters. Our initial conditions mirror those of PZ01, except that in some cases, our stars begin on the pre-main sequence rather than the zero age main sequence. In order to effectively determine the degree that adding pre-main sequence evolution affects a cluster simulation, we use the same input snapshots for the first three W6 models of PZ01, with various modifications outlined below.

For the input snapshots, PZ01 begin the simulation with 2048 nodes (single or binary stars) set up with a King (1966) model with a dimensionless depth (W_0) of 6, taking into account the velocity anisotropy and non-spherical shape that cluster would experience in the Galactic tidal field similar to that of Heggie & Ramamani (1995). The initial virial cluster radius was taken to be 2.5 pc. They then add a binary companion to every second node, for a total of 3072 stars. This is comparable to young clusters such as NGC 2516 and the Pleiades. Masses were applied to the nodes using a initial mass function prescribed by Scalo (1986) with masses ranging from 0.1 $M_\odot$ to 100 $M_\odot$, and a mean mass $\langle m \rangle \simeq 0.6 M_\odot$. This yields an initial total mass of $M_0 \sim 1600 M_\odot$, which is similar to estimates for the Hyades of Weidemann (1993). The masses for the secondary stars were selected randomly between 0.1 $M_\odot$ and the mass of the primary. The orbital eccentricities were selected from a thermal distribution between 0 and 1. The orbital separation a was selected with a uniform probability in log a, with a minimum separation of Roche lobe contact or 1 $R_\odot$, whichever is smaller. The maximum separation of the binaries was taken to be 10^6 $R_\odot$(about 0.02 pc). Note that the condition of Roche lobe contact implicitly includes some dependence the initial radius of the star. Finally, each star was assigned a radius, luminosity, and temperature based on their current evolutionary state. Main sequence initial prescriptions for radius, temperature, and luminosity are given by Eggleton, Fitchett, & Tout (1989). We

added pre-main sequence attributes (where applicable) using the tracks obtained from Siess, Dufour, & Forestini (2000).

We labeled our simulations as 'pz-ms', 'pz-pms' or 'rw-pms', with differences as follows. For our pz-ms runs, the snapshots were identical to those used in PZ01 – the positions, velocities, masses and other stellar and binary parameters were not changed. These runs were used for comparison purposes, since all stars in this set of simulations began their lives on the zero age main sequence. For our pz-pms runs, the positions, velocities, masses, and binary parameters were the same as those used in PZ01 but all low mass stars ($M \leq 7\mathrm{M}_{\odot}$) were started on the pre-main sequence birthline rather than on the zero age main sequence. Essentially the only initial condition that differed between the pz-ms and pz-pms runs was the stellar radius for low mass stars. The condition for chosing binary orbit separations was a limit based on Roche lobe contact, but pre-main sequence stars have much larger radii than zero age main sequence stars. Therefore, many of the binary systems in the pz-pms simulations were initially in contact. To address this issue, we also ran a third set of simulations (rw-pms) in which the positions, velocities and masses of stars were identical to PZ01, but the binary semi-major axes were re-assigned, with a limit based on Roche lobe contact as determined by the pre-main sequence radii. For each set of initial conditions, we ran three different realizations, corresponding to the first three realizations reported in PZ01. Where relevant, we label individual realizations as 'pz-pms1', etc.

Adding the pre-main sequence phase of evolution to the stars in our cluster highlights some confusion in dating clusters. What exactly is meant by an age of zero? If the pre-main sequence phase is included, then low mass stars will reach the zero age main sequence at different times, all of which are later than the start of the simulation, which we define as $T = 0$. In PZ01, it was clear that $T = 0$ corresponded to the moment when all stars are on the zero age main sequence. For our pre-main sequence simulations, we take $T = 0$ to be the moment when all stars are on the deuterium-burning birthline as defined by Palla & Stahler (1999) (see section 2.3). The difference between these two implementations is dependent on the mass of star in question. When comparing ages from dynamical simulations to those determined from observations, it is important to understand how the observed ages were derived.

2.2. Evolution

The entire system is evolved, including the effects of dynamics, individual stellar evolution, and binary evolution. For a complete description of all the computational techniques, the reader is directed to the descriptions of STARLAB, `kira`, and `SeBa` (McMillan 1996;

Portegies Zwart et al. 1999; Portegies Zwart & Verbunt 1996; Portegies Zwart & Yungelson 1998). In this section, we will concentrate on describing the numerical methods and parameters that were modified when we introduced the pre-main sequence phase of evolution.

Single star evolution from the zero age main sequence is based on the time-dependent mass-radius and mass-luminosity relations given by Eggleton, Fitchett, & Tout (1989). These relations are valid for the evolution of solar-metallicity stars on the main sequence, subgiant branch or Hertzsprung gap, giant branch, horizontal branch and asymptotic giant branch. Stars are immediately turned into inert remnants (white dwarf, neutron star or black hole) at the end of the asymptotic giant branch. The effective temperature and bolometric correction can be calculated for each star from the mass, radius and luminosity. Quantities such as core mass and mass loss due to a stellar wind are also parameterized, as outlined in Portegies Zwart & Verbunt (1996).

The evolution of the stars and binaries are computed with the `SeBa` binary population synthesis package (see Portegies Zwart & Verbunt, 1996, Sect. 2.1 with changes made in model B of Portegies Zwart & Yungelson, 1998). In this synthesis model the two stars in a binary are evolved synchronously updating each of the stars at regular intervals while keeping track of the changes to the orbital period and eccentricity. The simulation model includes various stability criteria for mass transfer, tidal circularization, the emission of gravitational waves, supernova explosions, etc.

2.3. Treatment of Pre-main Sequence Stars

For our pre-main sequence recipes, we looked to the evolutionary tracks of Siess, Dufour, & Forestini (2000), a selection of which are shown in figure 1. They give pre-main sequence tracks that begin with a fully convective protostar, and end just after hydrogen burning begins. Their tracks have resolution in mass of 0.1 $M_\odot$ from 0.3 to 2 $M_\odot$, higher mass resolution between 0.1 and 0.3 $M_\odot$, and lower resolution between 2 and 7 $M_\odot$. We used the tracks for a metallicity of $Z = 0.02$ (i.e. solar metallicity, appropriate for young open clusters) and used the portions of their tracks which begin at the pre-main sequence birthline described by Palla & Stahler (1999) and end at the zero age main sequence. We did not implement the pre-main sequence phase for stars with masses greater than 7 $M_\odot$ because these stars spend little or no time on the pre-main sequence. We combined all the tracks to create a lookup table in which we interpolated linearly through mass and age to find radius and temperature.

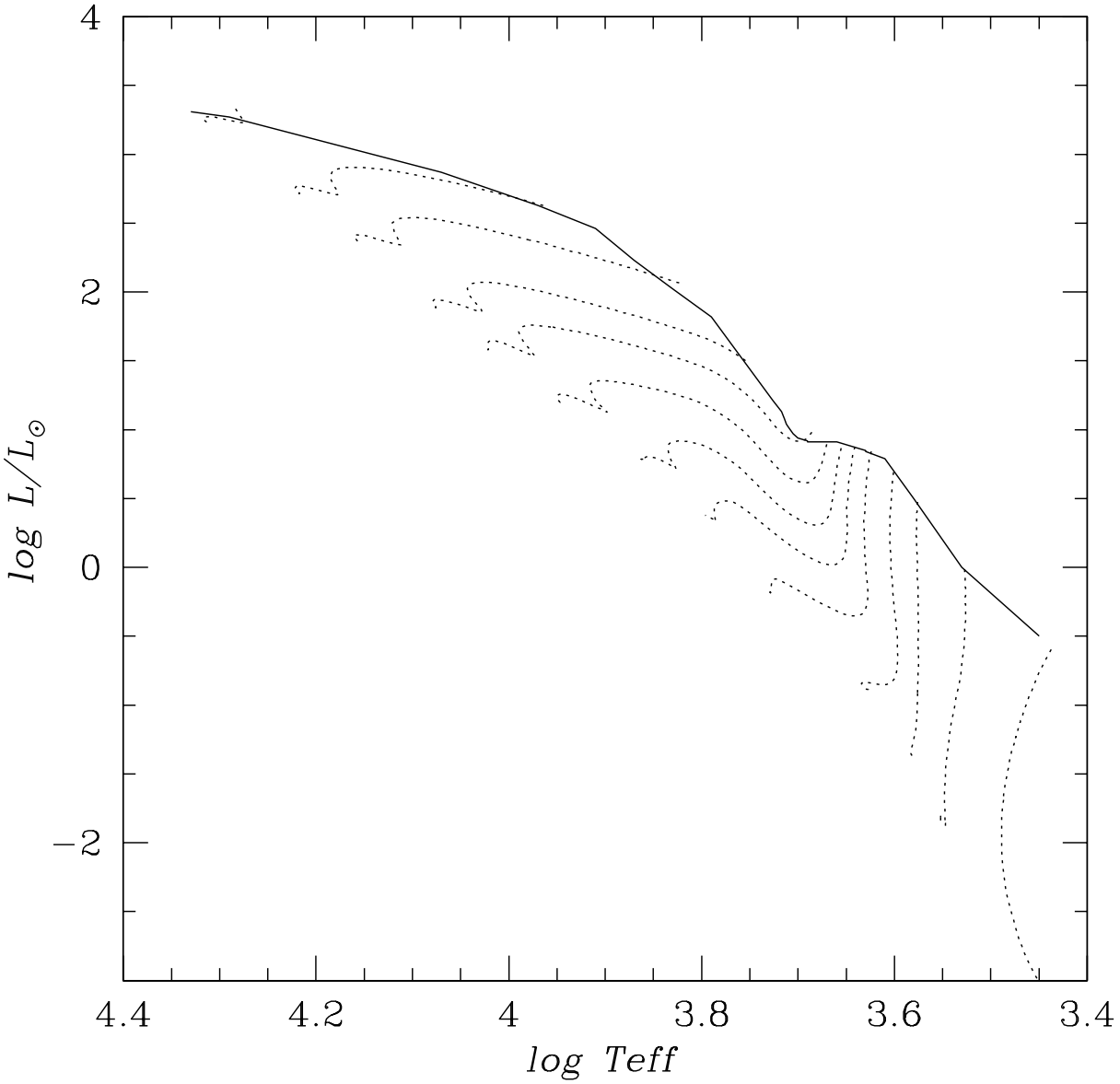

Fig. 1.— Pre-main sequence tracks of Siess, Dufour, & Forestini (2000), showing the region between the birthline of Palla & Stahler (1999) (solid line) and the zero age main sequence. The masses shown are 0.1, 0.3, 0.5, 0.7, 1.0, 1.3, 1.6, 2.0, 2.5, 3.0, 4.0, 5.0 and 7.0 $M_\odot$

Although other pre-main sequence tracks exist (D'Antona & Mazzitelli 1997; Palla & Stahler 1999), we chose to use the Siess, Dufour, & Forestini (2000) tracks. They have sufficient resolution and span the entire range of masses to which pre-main sequence evolution applies. Since theoretical tracks from different authors differ amongst themselves it was important to be able to have enough data to infer the properties of the star for a given mass and age. The range of masses is quite appropriate since our initial mass function has a lower limit of 0.1 $M_\odot$, and stars with masses higher than about 7 $M_\odot$ do not have a significant pre-main sequence phase. Another reason we chose these tracks was that they had data for stellar radius and temperature that were easily manipulated. Siess, Dufour, & Forestini (2000) compare their tracks with others and find good correspondence with most other tracks, although there is still some debate concerning the form of very low ($M \leq 0.4$ $M_\odot$) mass pre-main sequence evolution.

Beyond temperature, radius and luminosity, a number of other parameters need to be specified for pre-main sequence stars. These parameters come in two categories: those dealing with single-star evolution, and those dealing with binary evolution. Unfortunately, many of these parameters have not been determined for pre-main sequence stars. To make reasonable choices, we had to look to stars with similar composition (main sequence) or similar structure (the large convective envelope of a giant) to give us these other characteristics. For instance, the way that we chose to calculate the mass transfer and age rejuvenation from accreting binary star systems in STARLAB is similar to the main sequence recipes, but the parameters controlling mass transfer relations are based on the values for giant stars. Similarly, we took the value for the radius of gyration to be that of giant stars. Since pre-main sequence stars do not exhibit mass loss (especially stars with masses less than 7 $M_\odot$), we neglected stellar winds on the pre-main sequence.

One of the major benefits of using the STARLAB environment is that there are prescriptions for mergers or collisions of varying types of stars. Collisions and mergers can be distinguished in that a merger is a result of unperturbed binary evolution, and is preceded by a period of mass transfer. Currently, the code does not treat collisions that do not result in a merged object, so at the moment when the two stars are replaced by a single star the result will depend only on the types of stars and their mass.

Encounters involving main sequence and post-main sequence stars are described in PZ01. The merger of two main sequence stars is treated as conservative mass accretion from the less massive secondary to the more massive primary. This results in a rejuvenation of the star – which usually is observed as a blue straggler if the masses of the stars are large enough, or as a reasonably normal main sequence stars if the total mass of the new object is less than the current turnoff mass. The merger of other types of stars result in evolved stars or

unusual objects, as warranted by the structure of the two stars involved in the collision.

The treatment of encounters involving pre-main sequence stars was similar to the treatment of main sequence stars – when a pre-main sequence star collided with a more evolved star, the result was taken to be similar to the result of a main sequence star colliding with the same kind of star. For pre-main sequence/pre-main sequence collisions, the merged object was returned to the pre-main sequence birthline as its evolutionary state will be completely disrupted. These choices are in agreement with the results of the hydrodynamic simulations of Laycock & Sills (2005) of collisions involving pre-main sequence stars.

3. Results

3.1. Global Cluster Properties

Two of the most general functions that represent the time evolution of star cluster are its total mass and total number of particles versus time. The processes which can decrease the total number of cluster members are a merger between two stars, type Ia supernovae (which do not leave a remnant) and the escape of a star from the system. Stars may escape as a result of a mixture of influences: dynamical encounter with a binary, supernova kick, or removal by the galactic tidal field.

Figure 2 shows the total number of stars (where a binary system counts as 2 stars) versus time for each set of runs. The largest effect is the large initial drop in the number of stars in the pz-pms runs (dashed line). This has mainly to do with early mergers that occur within these clusters. In these runs, all of the binaries that had a small orbital separation in the main sequence configuration are now in contact. As a result, a large number of binaries merge immediately after initialization of the simulation. Eventually, the evidence of this event is erased, and the number of remaining cluster members approaches that of the other series. The rw-pms runs experience a decreased number of mergers throughout the life of the cluster since the radii of the stars become smaller throughout the pre-main sequence lifetime, and may only reach a point of Roche lobe overflow when one of the stars becomes a giant. As a result, the rate of decrease of the number of stars for the rw-pms runs (-1.5 stars/Myr) is lower than the rate the pz-ms runs (-1.6 stars/Myr), but with a very similar slope to the pz-pms runs (-1.44 stars/Myr). The slopes were measured between 500 and 1500 Myr. This dependence of the dynamical results on the initial binary merger rate highlights the most important conclusion of this paper. The inclusion of pre-main sequence stars in dynamical simulations affects only the binary properties of the system, and a consistent treatment of the pre-main sequence binary population is necessary.

The evolution of the total mass of the cluster is driven by two processes. One is mass loss from stars via stellar winds, and the other is the escape of stars from the cluster. The differences caused by including the pre-main sequence phase are quite small, as shown in figure 2. The maximum difference between the total mass of the pz-ms run and both pre-main sequence runs is at most 6%.

Table 1: Number Loss and Mass Loss at 1.5 Gyr for all runs

	pz-ms	pz-pms	rw-pms
% of stars that have escaped	65 ± 4	60 ± 5	60 ± 10
% objects that have merged	3.1 ± 0.5	15 ± 2	0.4 ± 0.2
% total mass lost via escapers	48 ± 4	45 ± 5	45 ± 5
% total mass lost via stellar winds	19 ± 3	20 ± 3	19 ± 3

Table 1 summarizes which modes of mass loss and number loss are experienced in each of the models. The error bars on each number give an indication of the range between different realizations of each set of initial conditions. Within the errors, the same number of stars escape from the cluster in all runs since the escape processes are driven by stellar dynamics, which is most influenced by the masses of the stars and binaries, and which is hardly affected by the pre-main sequence evolution. As noted above, the number of mergers is much higher in the pz-pms runs because of the combination of the initial orbital semi-major axes and the larger pre-main sequence evolutionary radii. These mergers cause the average individual stellar mass to increase slightly. However, there is no noticeable change in the amount of mass lost through stellar winds because stars that exhibit the pre-main sequence phase have masses of less than 7 $M_\odot$. Therefore, the high-mass stars which exhibit significant mass loss ($M \gtrsim 25$ $M_\odot$) will have their masses increased by a very small amount, which will not dramatically change the amount of mass loss due to stellar evolution for the cluster. Recall that high-mass stars do not have pre-main sequence evolutionary tracks, and therefore are unaffected by the changes made in this paper.

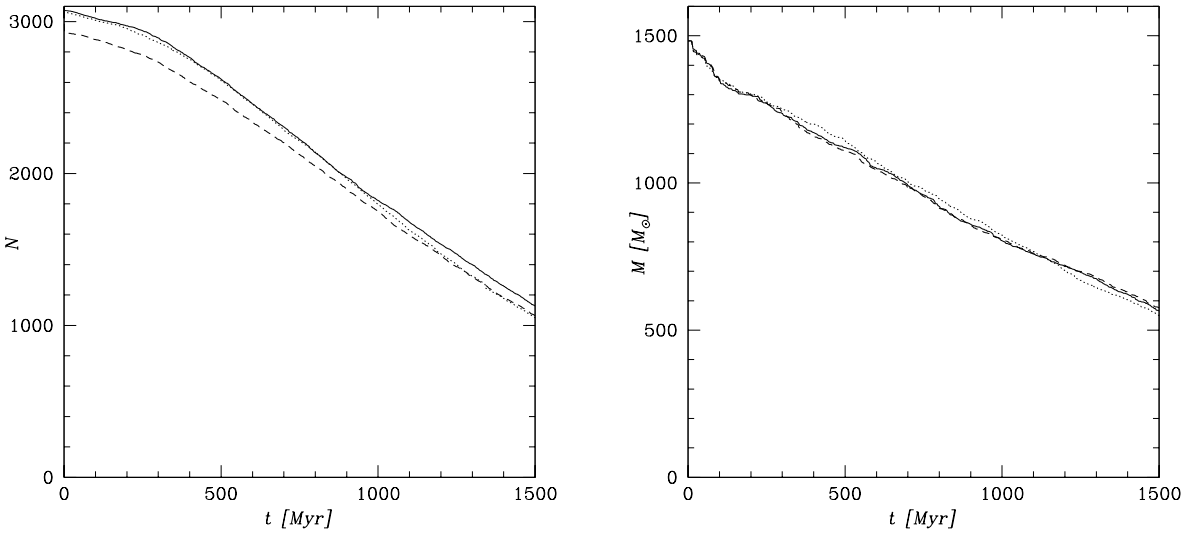

Fig. 2.— Total number of stars in the cluster averaged all runs (left), and total mass of run 1 (right). Results shown are from the pz-ms (dotted), pz-pms (dashed), and rw-pms (solid) sets of simulations.

Figure 3 shows how density in the core and at the half-mass radius of the cluster changes with time for the different models. The overall density of the clusters seem to stay the same, but at around 1.2 Gyr, the cores of the pz-ms and pz-pms clusters continue to decrease in density, while the density in the core of the rw-pms runs becomes approximately constant. This may indicate that the core of these clusters can still absorb energy as massive stars fall toward the center and low mass stars are ejected, and is related to the number and hardness of binaries in the core (Merritt et al. 2004).

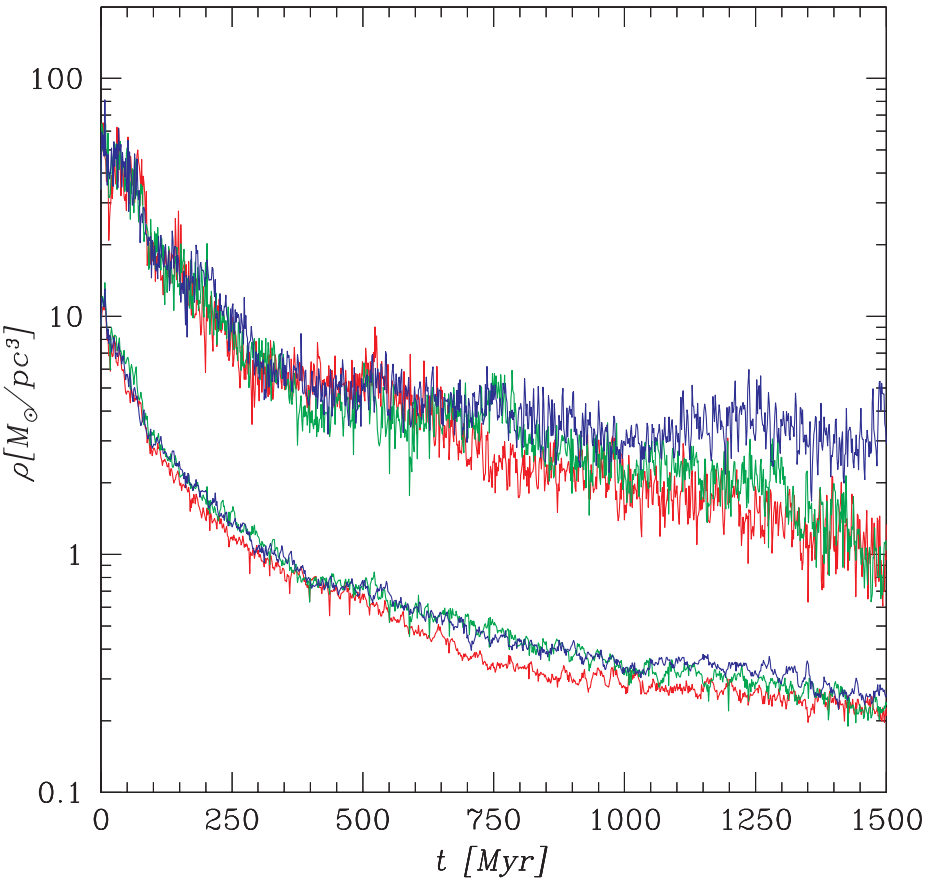

Fig. 3.— Stellar density versus time averaged over all realizations of models pz-ms (red), pz-pms (green), and rw-pms (blue). The top and bottom lines represent the density within the 10% and 50% Lagrangian radii respectively.

We see evidence for mass segregation in all our runs, as seen in figure 4, a plot of the average stellar mass within various Lagrangian radii as a function of time. The average mass in the pz-pms and rw-pms runs increase dramatically at first, and then level off to a value slightly above the pz-ms runs. The average mass inside the 5% Lagrangian radius, averaged between $T = 0$ and $T = 1500$ Myr, for the three runs are 1.00 ± 0.07 $M_\odot$ for the pz-ms run and 1.00 ± 0.04 $M_\odot$ for the pz-pms run but 1.2 ± 0.1 $M_\odot$ for the rw-pms run. Again, the initial mergers that the pre-main sequence stars experience result in masses higher than normal, yielding a higher average mass especially in the innermost region of the cluster.

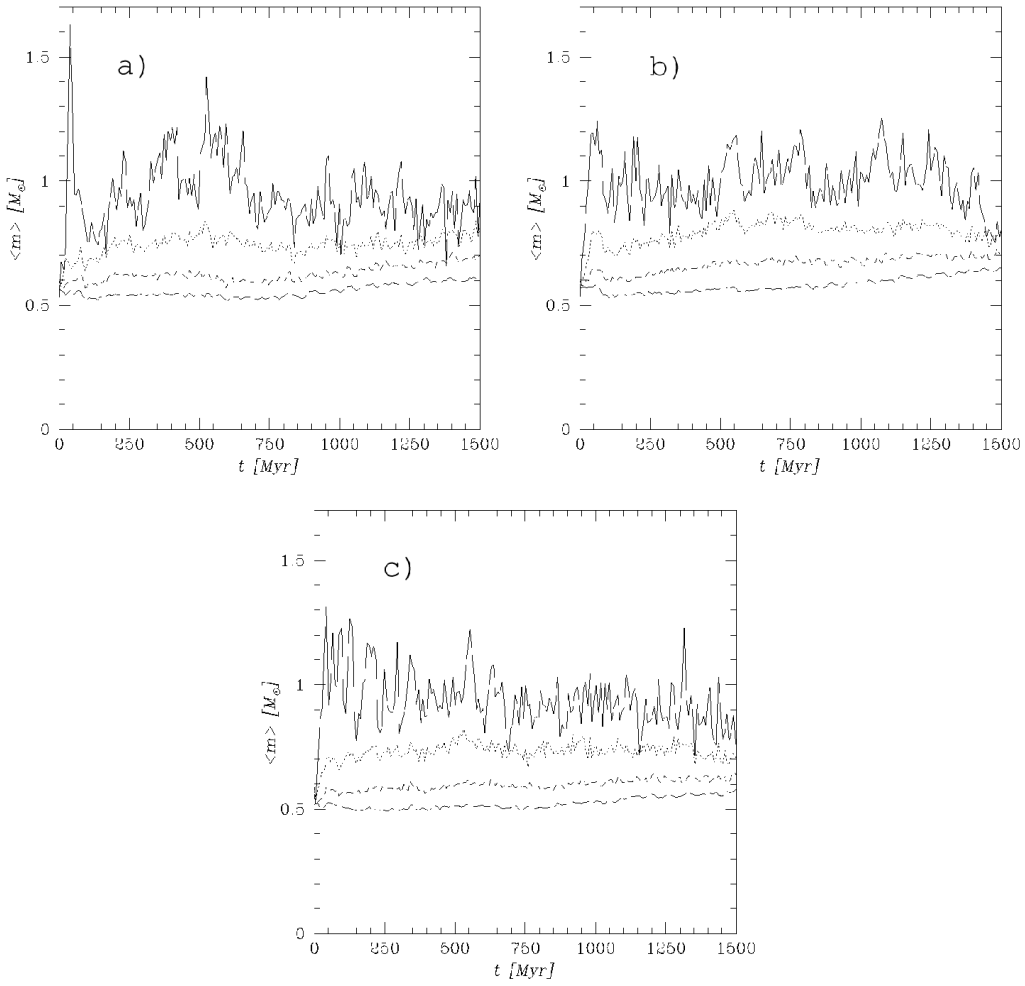

Fig. 4.— Average stellar mass versus time for pz-ms1 (panel a), pz-pms1 (panel b), and rw-pms1 (panel c). Shown are the average mass calculated inside the 5% (top line), 25%, 50%, and 75% (bottom line) Lagrangian radii. The values were smoothed over 7.5 Myr intervals.

Figure 5 shows the evolution of the mass and luminosity functions over time in our simulations. The runs in which the stars begin on the pre-main sequence have an initial luminosity function which is strongly weighted towards bright stars, as expected. After 600 Myr these models still do not fill the low luminosity bins because the lowest mass stars still have not evolved onto the main sequence. In the mass function diagram, the pz-ms1 and rw-pms1 models evolve similarly, with the pz-pms1 model having fewer low mass stars (mainly due to a high number of early mergers). A Kolmogorov-Smirnoff test cannot distinguish between the various mass functions at the 97% level. The luminosity functions of the two pre-main sequence runs (pz-pms and rw-pms) after 600 Myr are drawn from the same distribution to within 99.8%, while the pz-ms and rw-pms luminosity functions give a KS probability of 89% (i.e. only marginally different). As is expected, the two initial luminosity functions have only a 13% probability of being drawn from the same distribution. Therefore, it would appear that after only 600 Myr, most of the observational differences between the two treatments of starting point for the cluster stars have been erased. This is not a surprise, since the cluster is a few initial half-mass relaxation times old, so one would expect that small changes to the initial conditions or to the early stellar evolution have been erased.

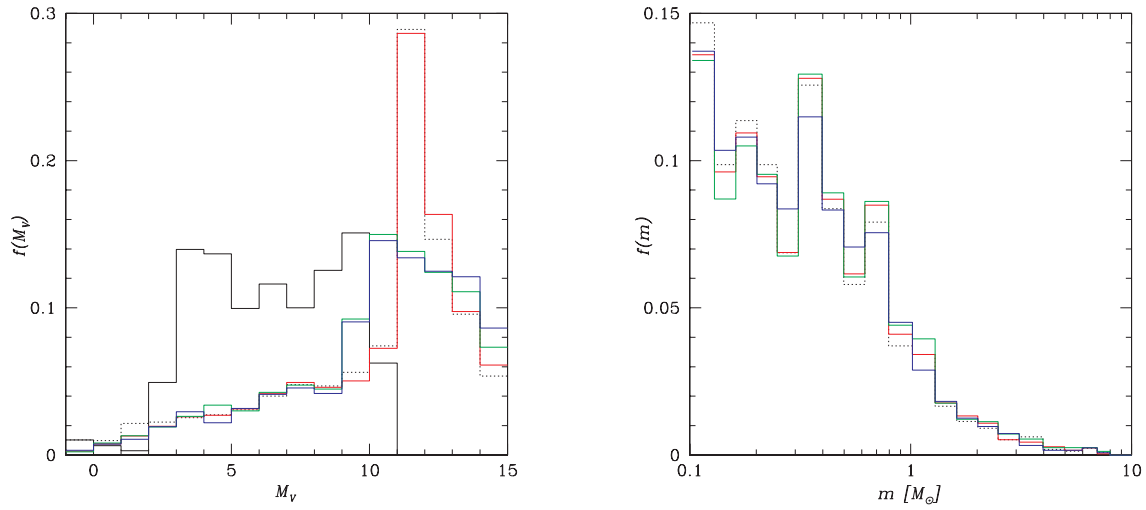

Fig. 5.— Luminosity (left) and mass (right) functions for models pz-ms1, pz-pms1, and rw-pms1. The dotted line represents the initial configuration for the pz-ms run (which is identical to the models starting on the pre-main sequence for the mass function) and the solid black line represents the initial configuration for the pz-pms run and the rw-pms run. Also shown are the data at 600 Myr for pz-ms (red), pz-pms (green), and rw-pms (blue).

In figure 6 the time evolution of the colour-magnitude diagram (CMD) of the cluster is shown. Features such as the binary main sequence, blue stragglers, and a collection of giants and white dwarfs are clearly visible. The pre-main sequence stars begin above the main sequence and descend down towards the main sequence. In the more evolved colour-magnitude diagrams, a gap is noticeable in the main sequence for the rw-pms and pz-pms simulations. A similar gap has been observed in NGC 3603 (Eisenhauer et al. 1998) at a mass of about 4 $M_{\odot}$. Since NGC 3603 is less than 5 Myr old, the gap should continue to move down the zero age main sequence as the cluster ages. The gap itself is a result of non-linearities in the mass-absolute magnitude relation. These non-linearities arise from CNO burning that is initially out of equilibrium in pre-main sequence stars (Piskunov & Belikov 1996). Another notable feature of the CMDs is that the binary main sequence is more sparsely populated in the pz-pms1 run. This is another result of the increased number of early binary mergers, which results in a reduced binary fraction in these runs.

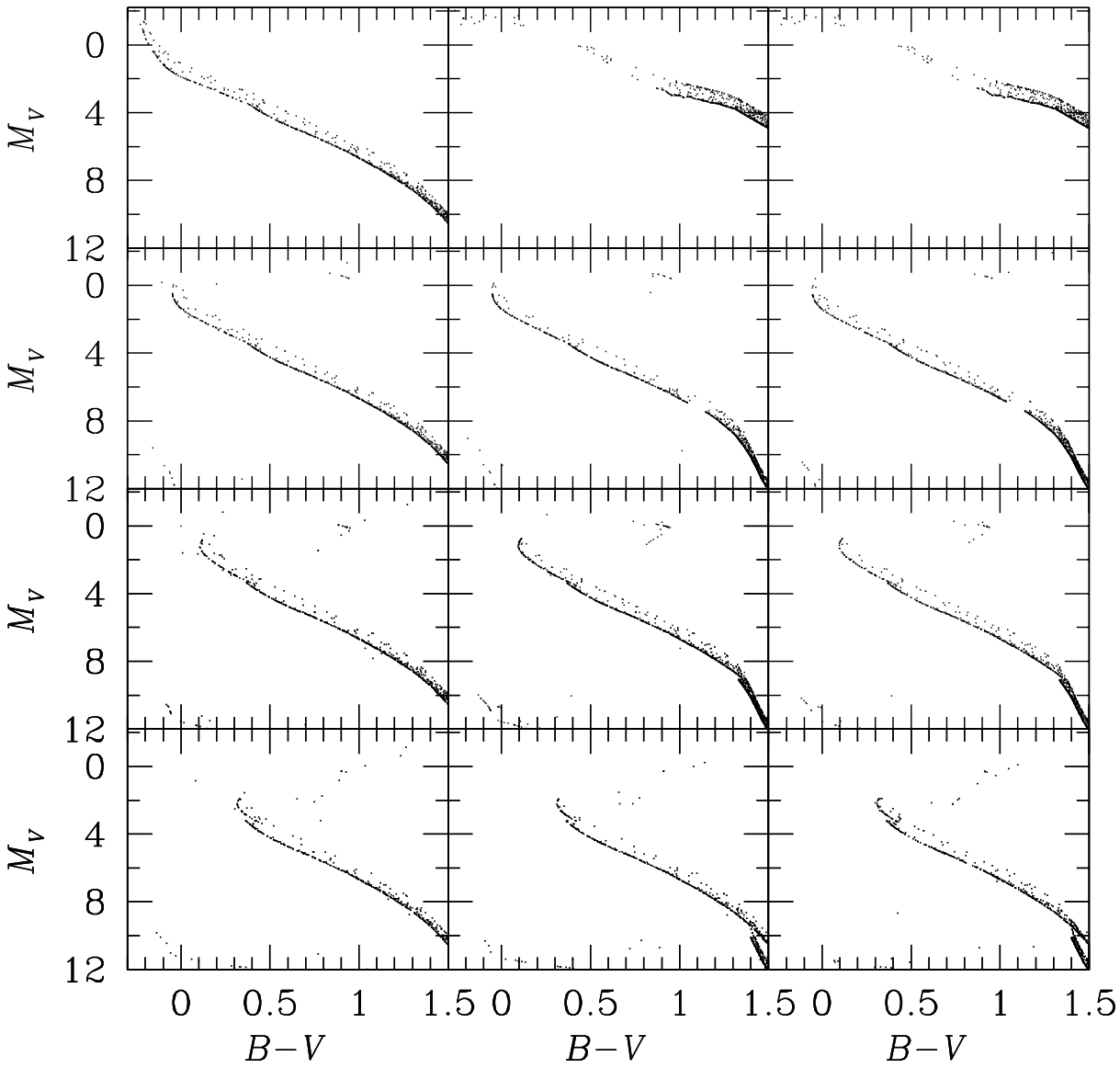

Fig. 6.— Colour-Magnitude Diagrams (CMDs) for models pz-ms1 (left), pz-pms1 (center), and rw-pms1 (right). Descending chronologically, the CMDs shown represent the clusters at approximately 0, 300, 600, and 1200 Myr.

3.2. Local Stellar Properties

The stellar populations in the various runs are quite different. Pre-main sequence stars are quite numerous throughout the lifetime of each of the clusters starting at the pre-main sequence. Aside from that, there is a slight decrease in the number of stellar remnant and giant stars. Tables 2, 3 and 4 show the time evolution of the various populations (single stars and binaries) in the cluster. Here and throughout, 'pms' stands for pre-main sequence star, 'ms' stands for main sequence star, 'gs' stands for giant star, and 'rm' stands for stellar remnant. Each table was created by averaging the results over three different realizations of the initial conditions. The differences between the tables are due to true differences between calculations, since each set of runs used identical realizations of the initial snapshots, and only the initial evolutionary state of the stars (zero age main sequence or pre-main sequence) and the binary orbital properties were changed, as outlined above.

Almost all of the features seen in tables 2 – 4 are attributable to either the difference in the number of mergers or the shift in age that the entire population experiences due to starting on the pre-main sequence. The fact that the lower mass stars start their main sequence evolution later results in a non-uniform shift in the population. It is interesting to note that in many instances, the pz-ms runs sit in between the ps-pms and rw-pms runs. For instance, the number of white dwarfs in the pz-ms runs stays steadily between the rw-pms and the ps-pms runs. The reason that there are so many white dwarfs in the pz-pms runs with respect to the rw-pms runs is that the merger products from early in a pz-pms cluster's lifetime will have a high mass, and thus tend to move more quickly to the remnant stage.

Table 2: Population Evolution of pz-ms Runs

time [Myr]:	0	100	200	400	600	800	1000	1200
ms	1024	1407.7	1374.3	1251.0	1109.0	931.7	763.3	610.7
gs	0	4.0	6.3	7.3	9.0	7.0	8.0	5.7
rm	0	7.0	14.0	27.0	39.7	48.0	51.0	53.3
ms/ms	1024	788.3	766.0	714.7	628.7	554.3	464.7	377.0
ms/gs	0	0.6	1.3	1.3	3.3	2.7	2.0	2.3
ms/rm	0	0.6	3.3	5.0	4.3	7.0	9.0	9.7
gs/gs	0	0.0	0.3	0.0	0.0	0.0	0.7	0.0
gs/rm	0	0.0	0.6	1.3	0.7	0.7	0.7	1.0
rm/rm	0	0.0	0.6	3.3	3.3	4.0	5.0	3.3

Table 3: Population Evolution of pz-pms Runs

time [Myr]:	0	100	200	400	600	800	1000	1200
pms	1020.3	1395.3	1274.7	1071.0	868.7	684.7	524.3	379.7
ms	3.7	144.7	219.0	288.3	320.0	333.3	320.3	302.3
gs	0.0	3.7	5.7	6.3	7.7	8.3	8.7	7.0
rm	0.0	7.0	15.3	31.3	43.3	53.0	58.3	60.7
pms/pms	1020.6	600.7	553.3	473.3	392.7	322.3	258.3	200.3
pms/ms	2.7	34.7	56.0	74.3	86.0	85.3	85.0	75.7
pms/gs	0.0	0.3	0.0	0.3	0.0	1.0	1.0	0.3
pms/rm	0.0	0.0	0.3	0.3	0.3	0.3	1.0	1.7
ms/ms	0.7	23.7	28.7	45.0	55.0	59.3	61.7	62.0
ms/gs	0.0	0.3	1.7	0.7	2.7	1.0	0.7	1.3
ms/rm	0.0	0.0	1.7	3.0	4.0	5.3	5.7	5.7
gs/gs	0.0	0.3	0.0	0.0	0.3	0.0	0.0	0.0
gs/rm	0.0	0.0	0.7	0.7	0.3	0.7	0.3	0.3
rm/rm	0.0	0.0	1.7	2.0	1.7	2.0	1.7	1.3

Table 4: Population Evolution of rw-pms Runs

time [Myr]:	0	100	200	400	600	800	1000	1200
pms	1020.3	1450.0	1346.7	1148.3	936.3	735.7	566.0	471.7
ms	3.7	127.3	192.3	255.3	296.3	301.3	284.3	291.3
gs	0.0	4.3	5.0	3.7	7.7	7.3	8.3	8.7
rm	0.0	7.0	15.3	28.7	35.7	43.3	48.3	51.0
pms/pms	1020.6	643.0	600.0	512.3	418.7	334.7	262.3	226.7
pms/ms	2.7	44.3	61.0	87.3	95.0	104.3	100.3	97.3
pms/gs	0.0	0.0	0.3	1.0	0.3	1.7	0.7	0.3
pms/rm	0.0	0.0	0.3	0.7	2.0	1.7	2.7	3.3
ms/ms	0.7	22.3	32.7	47.0	56.3	64.3	67.7	66.7
ms/gs	0.0	0.0	2.3	1.7	2.3	0.3	1.0	1.0
ms/rm	0.0	1.3	1.3	4.7	6.0	7.7	6.7	6.3
gs/gs	0.0	0.0	0.0	0.0	0.3	0.0	0.0	0.0
gs/rm	0.0	0.0	0.0	0.3	1.3	0.3	0.3	1.0
rm/rm	0.0	0.3	1.0	2.3	3.0	4.7	5.0	4.0

In general, the different stellar populations end up being similarly distributed throughout the cluster. Figure 7 shows the cumulative radial distribution of all stars (panel a) and for main sequence stars only (panel b) at 600 Myr for the first run of each of the series. The radial distribution of all stars is almost identical for all three simulations, and this is also true for the individual populations of binary stars, giants, remnants, and pre-main sequence stars where relevant. The biggest difference is in the main sequence stars, as shown in panel b) of figure 7. The main sequence stars are significantly more centrally concentrated in the two runs with pre-main sequence evolution than in the pz-ms run. The main reason for this is that the lowest mass stars are still on the pre-main sequence. Therefore, the mean mass of main sequence stars is higher than that in the pz-ms run, and the population is more centrally concentrated.

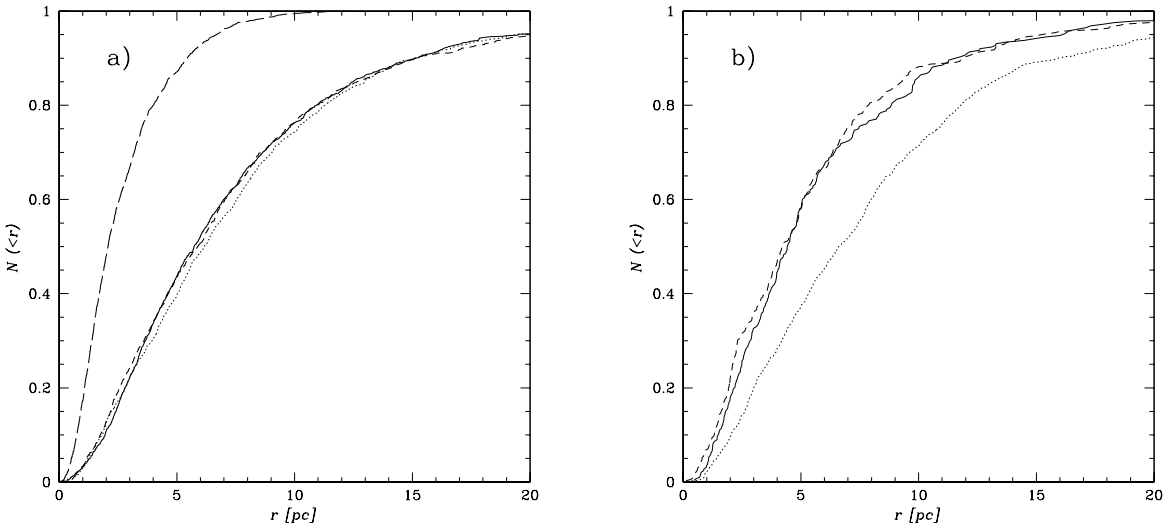

Fig. 7.— Radial distributions for runs pz-ms1 (dotted line) , pz-pms1 (short-dashed line), and rw-pms1 (solid line) at 600 Myr. Panel a) gives the radial distribution for all objects, while panel b) shows the radial distribution for main sequence stars only. The long-dashed line in panel a) shows the initial radial distribution of all objects.

Figures 8 and 9 show the binary orbital parameters (semi-major axis a and eccentricity e) of all stars at the start of the simulation and at 600 Myr for runs using the original binary orbits and using the more realistic binary orbits respectively. For the pz-pms simulation it is evident that almost all of the binaries with a small orbital period have merged or circularized by 600 Myr. For the rw-pms model almost no circularization occurs. This is again attributable to the fact that the pre-main sequence stars are contracting and are therefore rarely in a period where tidal effects are important. As is expected, all of the softer binaries (those with orbital periods larger than 10^4 yr) have been broken up in all models by 600 Myr. In addition, the pre-main sequence systems that are not initially in contact will only experience Roche lobe overflow after the terminal age main sequence when the star ascends the giant branch. Only then will these stars be larger than they were in their initial stage. Stars that are considered to begin their lives on the zero-age main sequence expand as they evolve, so there are more systems which experience Roche lobe overflow on the main sequence in the pz-ms runs.

We can directly compare the effects of including the pre-main sequence phase on binary evolution by making use of the information shown in figure 8. Both the pz-ms and the pz-pms runs started with the same 1024 binaries (those shown in the first panel). After 600 Myr, the pz-ms run has 639 binaries while the pz-pms run has only 545. However, only 426 systems are still in common between the two simulations. Of those 426, 300 have evolved in exactly the same manner and have exactly the same orbital elements. Many of those systems consisted of a pair of massive stars, and so were unaffected by the inclusion of the pre-main sequence phase in our simulations. The evolution of the other 126 systems is quite enlightening. We can calculate the total change in semi-major axes ($\Delta a = \Sigma_{\rm allbinaries} a_{\rm pz-ms} - a_{\rm pz-pms}$) and the equivalent quantity for eccentricity for the systems that are in common between the two simulations. The total change in semi-major axis is relatively small ($\Delta a = -150$ A.U. summed over 126 systems) and the differences are almost equally probable to be positive or negative. For comparison, the maximum binary semi-major axis in our simulations was 10^6 $R_\odot$, or $\sim$ 4600 A.U. The situation for eccentricity is quite different: $\Delta e = 45$. This very large number shows that the binaries in the ps-pms simulation are much more likely to have substantially lower eccentricities than the pz-ms run. This can be attributed to a phase of tidal circularization that occurs while the stars are on the pre-main sequence, and can be seen in the lack of high eccentricity systems in the third panel of figure 8.

It has been known for some time that there is a correlation between the age of a stellar population and the binary period below which all binaries in that population are circularized. This correlation is based on the efficiency of tidal circularization. However, the current models for circularization do not agree with all the available data (see Meibom & Mathieu (2005) for a recent review and investigation of this problem). We have shown in figure 8

that the tidal circularization period can differ by more than two orders of magnitude for two different assumptions about the properties of the initial starting point of the stars. Observations suggest that the tidal circularization period in the Hyades is 3.2 ± 1.2 days, or $\log P_{\rm orb}(\rm yrs) \sim -2$ (Meibom & Mathieu 2005). The pz-pms run is a much better fit to the data than the pz-ms run. In the rw-pms run, however, there are no binaries (either initially or after 600 Myr) with orbital periods that low. Once again, it is clear that understanding the initial binary properties on the pre-main sequence is crucial.

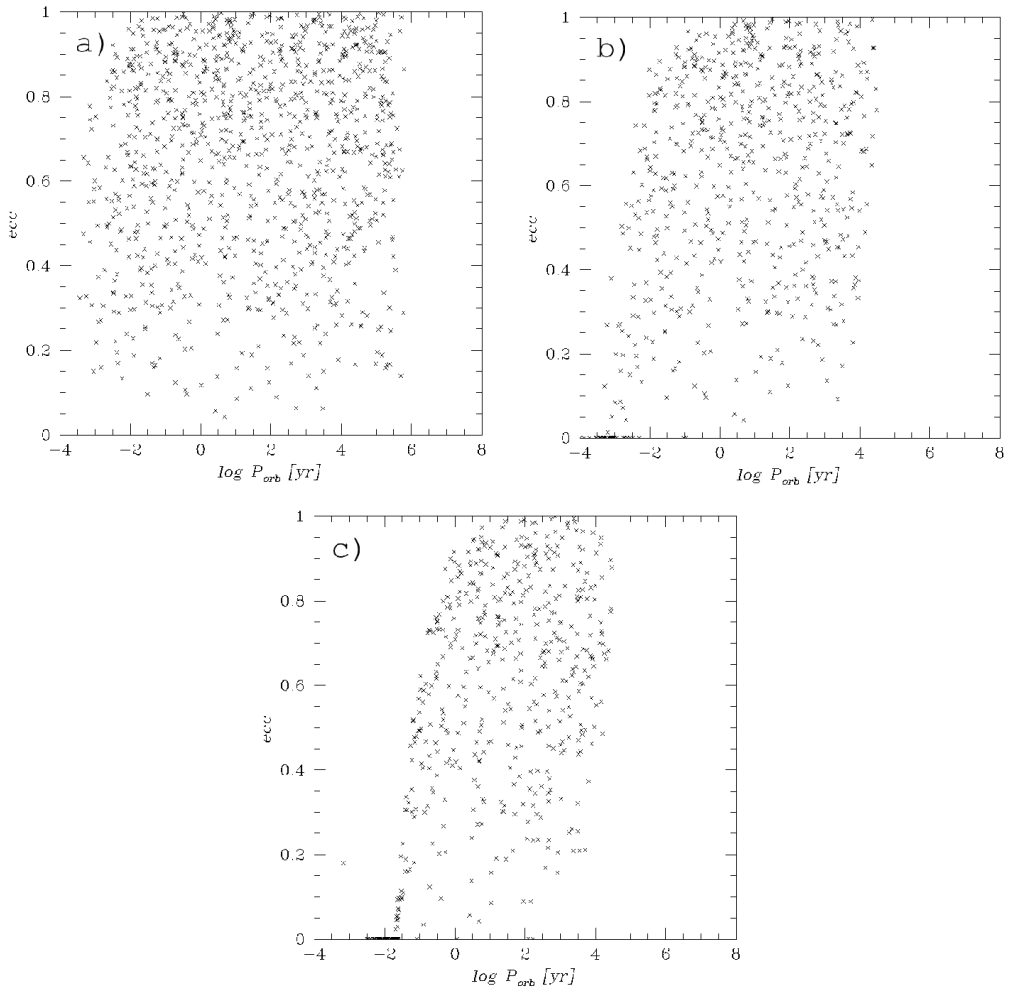

Fig. 8.— Eccentricity vs. orbital period of binaries for pz-ms1 and pz-pms1. Shown are the initial parameters shared by both runs (panel a), and the parameters at 600 Myr for pz-ms1 (panel b) and pz-pms1 (panel c).

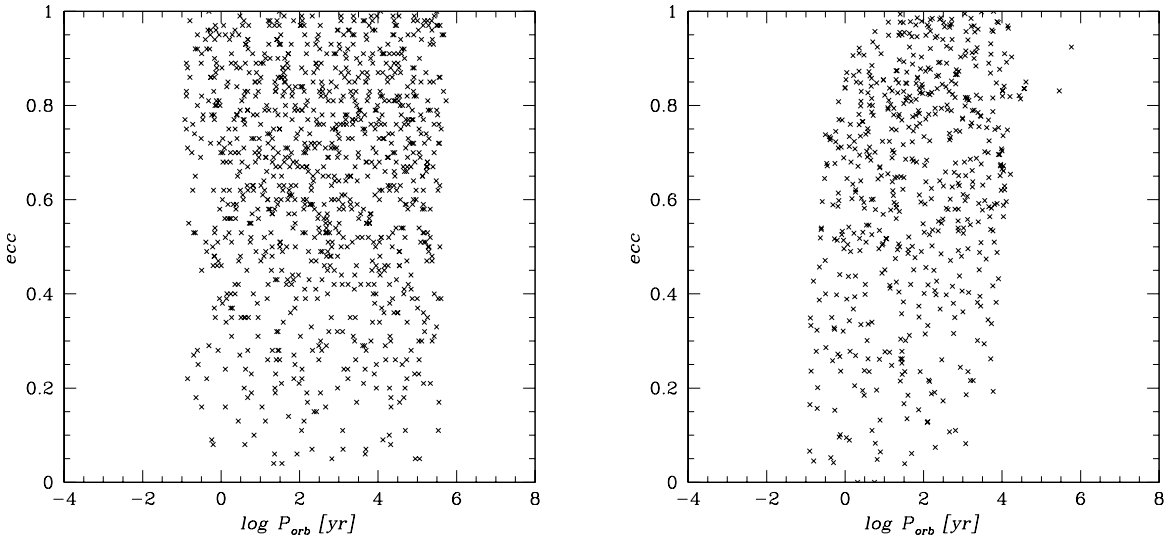

Fig. 9.— Eccentricity versus orbital period of binaries for rw-pms1. Shown are the parameters at 0 Myr (left) and 600 Myr (right).

Throughout the pz-pms and rw-pms runs, the binary fraction stays below that of the pz-ms runs, as seen in figure 10. The initial dip for the pz-pms runs is a result of the large number of mergers that occur within the first Myr after the simulation begins. For the rw-pms runs, the binary orbits were biased towards a higher fraction of soft binaries. This leads to many multiple systems breaking up into single stars early in the cluster's life. The binary fraction in both pre-main sequence simulations increases slightly with time because binaries are formed through stellar interactions in the core of the cluster, and because single stars are preferentially ejected from the cluster. The binary fraction within the inner 1 pc of the rw-pms cluster reaches about 75% after 600 Myr, and falls off steeply in the outskirts of the cluster. The number of very hard binaries ($E < -1000\,\mathrm{kT}$) is very small in the rw-pms run, making up no more than 6% of the binary fraction, compared to about twice that for the pz-ms run. Detailed observations of the binary properties in open clusters may therefore be able to constrain the initial binary properties in the cluster, if the observations are sufficiently complete and sufficiently precise to determine binary orbital parameters.

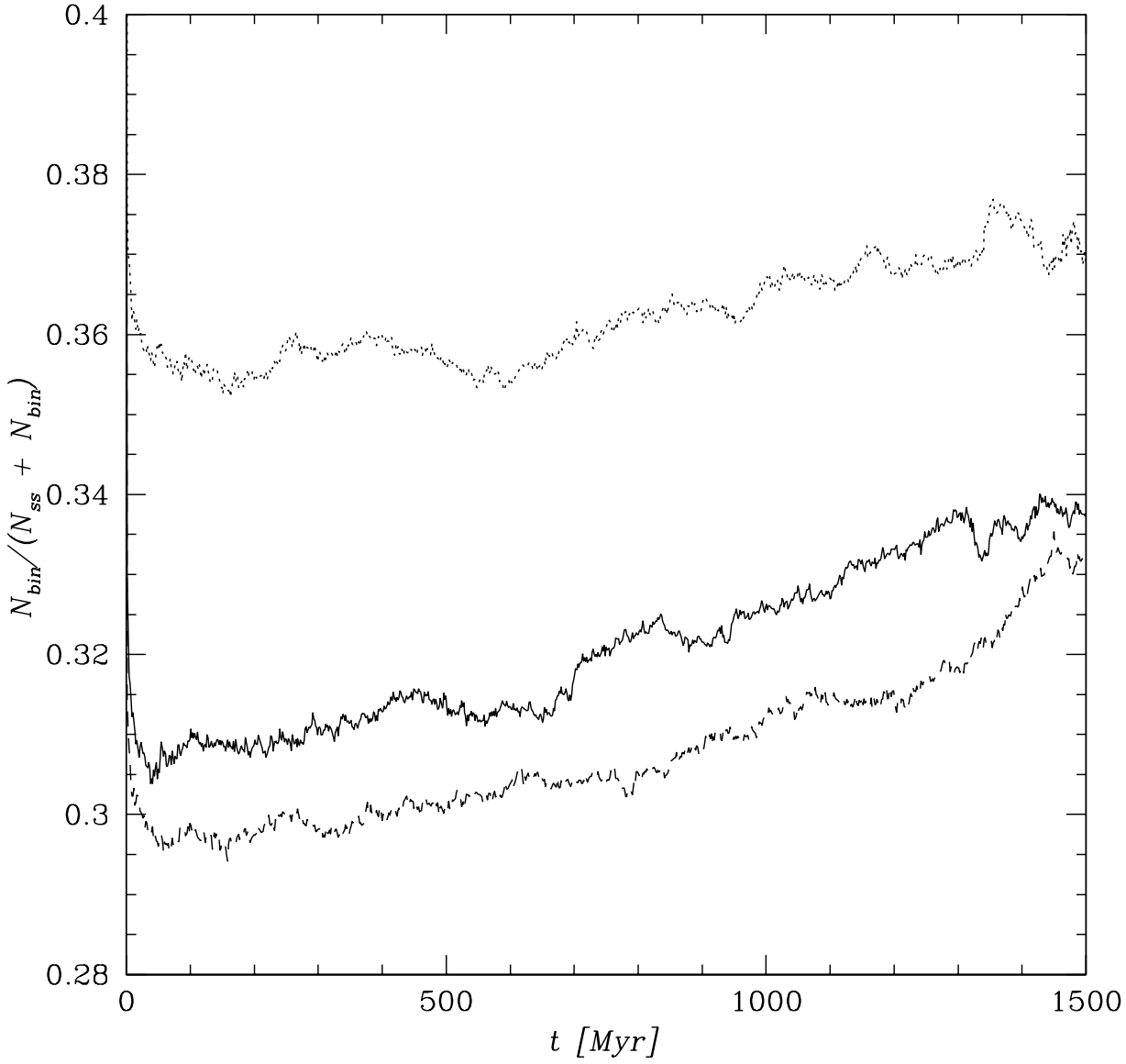

Fig. 10.— Binary fraction versus time for all binaries. Shown are pz-ms (dotted), rw-pms (solid),and pz-pms (dashed), averaged over all runs.

The most obvious and most important difference between runs of the pz-pms type and those of the other types are the number of mergers. In table 5 we give the total numbers of mergers seen in all simulations, sorted by kind of simulation. Because many of the binaries were in contact for the initial pz-pms conditions, the first timestep contained a very large number of mergers. On the other hand, the number of mergers for the rw-pms simulations was lower than that of the pz-ms simulations. This is because the binaries which included pre-main sequence stars started with large separations. The pre-main sequence stars then contracted towards their zero age main sequence radii, resulting in an increasing ratio of stellar radius to Roche lobe radius. These binaries will take longer to evolve towards Roche lobe contact than the binaries in the pz-ms runs, and Roche lobe overflow will happen after the star has started to ascend the giant branch. This is another indication that the most important thing to consider when including the pre-main sequence phase of stellar evolution is the initial parameters of binary systems in the cluster.

Table 5: Total number of different kinds of mergers for each run type.

Merger Type	PZ-MS	PZ-PMS	RW-PMS
pms/pms	0	441	0
pms/ms	0	0	1
pms/gs	0	5	7
ms/ms	86	1	1
ms/gs	8	1	0
ms/rm	4	2	1
gs/gs	1	0	0
gs/rm	7	7	1
rm/rm	2	2	1

4. Summary and Discussion

In this paper, we investigated the effects of allowing stars to begin their lives on the pre-main sequence in dynamical simulations. We added pre-main sequence evolutionary tracks which begin at the deuterium-burning birthline, and end at the zero-age main sequence. Stars with masses less than 7 $M_\odot$ in the dynamical simulations have their radii, luminosities, temperatures, and other properties determined by these tracks starting from the $T = 0$ point of the dynamical simulation. We compared these simulations with standard ones in which all stars begin their lives on the zero age main sequence at $T = 0$.

The dominant characteristic which distinguishes between our different initial conditions can be traced back to the number of mergers in the early stage of the cluster evolution. In the pz-pms runs, a lot of the binaries begin in Roche lobe contact, since the binary orbits are based on zero age main sequence radii, and pre-main sequence stars have much larger radii initially. These early pre-main sequence/pre-main sequence mergers show up as a decrease in the total number of stars, but an increase in average mass. This effect changes the mass function of the cluster, not only initially, but the effect continues to be noticed for quite a large portion of the cluster's lifetime (many tens of initial half-mass relaxation times). On the other hand, since the stars in the rw-pms runs start at a greater separation, and since the initial pre-main sequence radius is the largest radius for a given star until it becomes a giant star, there is an absence of mergers in these runs. This increases the binary fraction, and affects the mass function as well.

In spite of the initial drop of total number of objects in the pz-pms models, the time evolution of the total mass is not noticeably affected by the starting point of the stars. Similarly, the total number of stars in both pms simulations seem to decrease at a slower rate than their pz-ms counterparts. This is due to a smaller number of escapers ejected from the cluster through an encounter. The inclusion of pre-main sequence evolution causes the stellar interactions to be less violent. During a binary star/single star interaction, accretion during the stellar encounter affects the ensuing binary parameters which in turn affects the resulting ejection velocity. Indeed, the merger of close binaries (as in the pz-pms runs) or the absence of close binaries in the rw-pms runs should affect the cluster in the same way since binaries act as a heat sink for the total energy of the cluster. Since the predominant form of binary that stars in these models will encounter is not very hard, the heat sinks of the cluster can absorb more, thus decreasing the energy available for other purposes.

In the rw-pms models very little circularization is observed. This is because the stars are contracting away from each other, and therefore cannot maintain close proximity as required for circularization. The pz-pms runs contain the largest number of circularized binaries and has a tidal circularization period which best matches observations of the Hyades.

Another item of note is the frequency of the different types of mergers. Almost all of the mergers were due to the normal binary evolution in which a star's radius becomes large than its Roche lobe. The two most frequent mergers in the pms runs are pre-main sequence/pre-main sequence and pre-main sequence/giant star mergers (with the latter being more dominant in the rw-pms case). Hydrodynamic simulations of such collisions (Laycock & Sills 2005) suggest that the result will be a larger pre-main sequence star in the former case, and a larger giant star in the latter case.

There is a significant amount of future work that could be done in this area and could involve simulating other cluster configurations (for instance, with more stars or in different tidal field). Since pre-main sequence stars in very young clusters have been studied (e.g., Eisenhauer et al. (1998)), a focus on the first 100 Myr of a simulation could be insightful. Another avenue of research would be to perform population synthesis in order to better determine which initial distribution of binary parameters will result in the observed distribution of these parameters, along the lines of Kroupa (1995). Both the choices for initial binary orbits in the rw-pms and pz-pms runs were quite simplistic and should be improved upon.

There are two noteworthy pieces of astrophysics that we have completely neglected from these simulations. Both are particularly relevant to the study of young clusters, particularly clusters significantly younger than the 600 Myr Hyades analogue we concentrated on here. The first topic is the inclusion of the gas out of which the stars in these clusters formed. We know from observations of star forming regions that there is a reasonably long period of time when both stars and gas co-exist, and are presumably interacting dynamically. We neglect that stage completely by starting with a stars-only King model. The second topic is the effect of circumstellar (and circumbinary) disks around the young stars in the cluster. Interactions between stars with disks should be slightly different than interactions between stars without disks, and could modify our results. In this paper, we have demonstrated that the careful treatment of cluster initial conditions is important, and there are clearly other avenues for improvement as well.

Our conclusion from this study is that inclusion of the pre-main sequence phase of stellar evolution is critical for any simulations that wish to understand the properties of binary stars in stellar systems. The choice of initial binary parameters and their subsequent evolution are strongly modified by the properties of pre-main sequence stars.

RW acknowledges support from SHARCNet. AS is supported by NSERC and the Canadian Foundation for Innovation. SPZ acknowledges support from the Dutch Royal Academy of Science (KNAW), Dutch Organization for Scientific Research (NWO) and Dutch Research

School for Astrophysics (NOVA).

REFERENCES

Aarseth, S. J. 1971, Ap&SS, 13, 324

Aarseth, S. J. 1996, IAU Symp. 174: Dynamical Evolution of Star Clusters: Confrontation of Theory and Observations, 174, 161

D'Antona F. & Mazzitelli I., 1997, Mem. Soc. Astron. Italiana, 68, 807

de la Fuente Marcos, R., & de la Fuente Marcos, C. 2002, Ap&SS, 280, 381

Duquennoy, A. & Mayor, M., 1991 A&A, 248, 485

Eggleton P. P., Fitchett M. J., & Tout C. A. 1989, ApJ, 347, 998

Elson R., Hut P., & Inagaki S. 1987, A&A Rev., 25, 565

Eisenhauer F., Quirrenbach A., Zinnecker H., & Genzel R. 1998, ApJ, 498, 278

Garcia Lopez R. J., Rebolo R., & Martin E. L. 1994, A&A, 282, 518

Heggie D. C. & Ramamani N. 1995, MNRAS, 272, 317

Hills, J. G. 1975, AJ, 80, 1075

Hurley J. R., Pols O. R., & Tout C. A. 2000, MNRAS, 315, 543

Hurley J. R., Tout C. A., Aarseth S., J., & Pols O., R. 2001, MNRAS, 323, 630

Hut, P., & Inagaki, S. 1985, ApJ, 298, 502

Hut, P., et al. 2003, New Astronomy, 8, 337

King I. R. 1966, AJ, 71, 64

Kouwenhoven, M. B. N., Brown, A. G. A., Zinnecker, H., Kaper, L., & Portegies Zwart, S. F. 2005, A&A, 430, 137

Kroupa, P. 1995, MNRAS, 277, 1491

Kroupa P., Gilmore G., & Tout C. A. 1991, MNRAS, 251, 293

Kroupa P., Tout C. A., & Gilmore G. 1993, MNRAS, 262, 545

Laycock, D., & Sills, A., 2005, ApJ, 627, 277

Makino, J., Fukushige, T., Koga, M., & Namura, K. 2003, PASJ, 55, 1163

Mathieu, R. D., & Latham, D. W. 1986, AJ, 92, 1364

McMillan, S. L. W. 1996, ASP Conf. Ser. 90: The Origins, Evolution, and Destinies of Binary Stars in Clusters, 90, 413

Merritt, D., Piatek, S., Portegies Zwart, S., & Hemsendorf, M. 2004, ApJ, 608, L25

Meibom, S., & Mathieu, R. D. 2005, ApJ, 620, 970

Palla F., & Stahler S. 1999, ApJ, 525, 772

Piskunov A. E., & Belikov, A. N. 1996, Astronomy Letters, 22, 466

Portegies Zwart, S. F., & Verbunt, F. 1996, A&A, 309, 179

Portegies Zwart, S. F., & Yungelson, L. R. 1998, A&A, 332, 173

Portegies Zwart, S. F., Makino, J., McMillan, S. L. W., & Hut, P. 1999, A&A, 348, 117

Portegies Zwart S. F., McMillan, S. L. W., Hut P., & Makino J., 2001, MNRAS, 321, 199

Portegies Zwart, S. F., Baumgardt, H., Hut, P., Makino, J., & McMillan, S. L. W. 2004, Nature, 428, 724

Scalo J.M. 1986, Fund. of Cosm. Phys., 11, 1

Schaerer, D., de Koter, A., Schmutz, W. & Maeder, A., 1996, A&A, 310, 837

Siess L. Dufour E. & Forestini M. 2000, A&A, 358, 593

Sills A., Deiters S., Eggleton P., Freitag M., Giersz, M., Heggie D., Hurley J., Hut P., Ivanova N., Klessen R. S., Kroupa P., Lombardi J. C. Jr., McMillan S., Portegies Zwart S., & Zinnecker H. 2003, New Astronomy, 8, 605

Sills A., Lombardi J. Jr., Bailyn C. D., Demarque P., Rasio, F. A., & Shapiro S. L. 1997, ApJ, 487, 290

Stauffer J. R., Jones B. F., Backman D., Hartmann L. W., Navascues D. B. Y., Pinsonneault M. H., Terndrup D. M., Muench A. A. 2003, AJ, 126, 833

Weidemann V. 1993, A&A, 275, 158